nature genetics

Loss of acetylation at Lys16 and trimethylation at Lys20 of histone H4 is a common hallmark of human cancer

Mario F Fraga[1], Esteban Ballestar[1], Ana Villar-Garea[1], Manuel Boix-Chornet[1], Jesus Espada[1], Gunnar Schotta[2], Tiziana Bonaldi[3], Claire Haydon[4], Santiago Ropero[1], Kevin Petrie[1], N Gopalakrishna Iyer[5], Alberto Pérez-Rosado[6], Enrique Calvo[7], Juan A Lopez[7], Amparo Cano[8], Maria J Calasanz[9], Dolors Colomer[10], Miguel Ángel Piris[6], Natalie Ahn[4,11], Axel Imhof[3], Carlos Caldas[5], Thomas Jenuwein[2] & Manel Esteller[1]

CpG island hypermethylation and global genomic hypomethylation are common epigenetic features of cancer cells. Less attention has been focused on histone modifications in cancer cells. We characterized post-translational modifications to histone H4 in a comprehensive panel of normal tissues, cancer cell lines and primary tumors. Using immunodetection, high-performance capillary electrophoresis and mass spectrometry, we found that cancer cells had a loss of monoacetylated and trimethylated forms of histone H4. These changes appeared early and accumulated during the tumorigenic process, as we showed in a mouse model of multistage skin carcinogenesis. The losses occurred predominantly at the acetylated Lys16 and trimethylated Lys20 residues of histone H4 and were associated with the hypomethylation of DNA repetitive sequences, a well-known characteristic of cancer cells. Our data suggest that the global loss of monoacetylation and trimethylation of histone H4 is a common hallmark of human tumor cells.

Epigenetics has become an increasingly important aspect of cancer biology. From the first observation of global genomic hypomethylation in tumors[1,2] to the identification of genes that are transcriptionally silenced in cancer cells by CpG island promoter hypermethylation[3–6] and the translational use of DNA demethylating agents[7], cancer epigenetics has focused mainly on aberrant DNA methylation. But changes in DNA methylation observed in transformed cells are not isolated events: they occur in the context of more complex epigenetic deregulation. DNA methylation is associated with the formation of nuclease-resistant chromatin[8], and DNA methyltransferases and methyl-CpG binding proteins are associated with histone deacetylases (HDACs) and histone methyltransferases[9,10]. This intimate relationship between DNA methylation and other components of the epigenetic layer, such as histones, is also expected to be disrupted in cancer cells.

Acetylation and methylation of lysine residues in the tails of nucleosomal core histones has a crucial role in chromatin packaging and gene expression[10,11]. Overall, histone hypoacetylation and hypermethylation is characteristic of DNA sequences that are methylated and repressed in normal cells[12,13]. Each lysine residue can be a marker for a different signal. In this regard, Lys16 of histone H4 (H4-Lys16) behaves differently from the other acetylated residues: its distribution is similar in the X chromosome and in autosomes[14]; it provides a barrier to the spreading of histone hypoacetylation and silencing[15]; and it is associated with differential binding of transcription factors[16]. The only lysine that is methylated in the tail of histone H4 is Lys20 (H4-Lys20). Trimethylation of H4-Lys20 is a marker of constitutive heterochromatin[17,18], gene silencing[17,18] and aging[19].

We are largely ignorant of how these histone modifications are disrupted in cancer cells. Hypermethylated promoter CpG islands of transcriptionally repressed tumor-suppressor genes are associated with hypoacetylated and hypermethylated histones[20–22]. Certain genes with tumor suppressor–like properties, such as *CDKN1A* (also called *p21*^{WAF1}), are transcriptionally silent, without CpG island hypermethylation, in association with hypoacetylated and hypermethylated histones[23,24]. But no profile of overall histone modifications and their genomic locations in the transformed cell has been identified. It is important to determine this histone modification pattern, because HDAC inhibitors are being developed as anticancer drugs[25]. Here, we comprehensively examined the modification patterns of histone H4 in human normal tissues and cancer cells.

[1]Cancer Epigenetics Laboratory, Molecular Pathology Program, Spanish National Cancer Center, Melchor Fernández Almagro 3, 28029 Madrid, Spain. [2]Research Institute of Molecular Pathology, The Vienna Biocenter, A-1030 Vienna, Austria. [3]Histone Modifications Group, Ludwig-Maximillians Universität München, Munich, Germany. [4]Department of Chemistry and Biochemistry, University of Colorado, Boulder, Colorado, USA. [5]Cancer Genomics Program, Department of Oncology, University of Cambridge, Hutchison/MRC Research Centre, Hills Road, Cambridge CB2 2XZ, UK. [6]Lymphoma Laboratory, Molecular Pathology Program, Spanish National Cancer Center, Madrid, Spain. [7]Proteomics Unit, Fundación Centro Nacional de Investigaciones Cardiovasculares, Madrid, Spain. [8]Biochemistry Department, School of Medicine, Universidad Autónoma de Madrid, Instituto de Investigaciones Biomédicas, Madrid, Spain. [9]Department of Genetics, School of Science, University of Navarra, Pamplona, Spain. [10]Hematopathology Unit, Hospital Clinic, University of Barcelona, Catalonia, Spain. [11]The Howard Hughes Medical Institute, Department of Chemistry and Biochemistry, University of Colorado, Boulder, Colorado, USA. Correspondence should be addressed to M.E. (mesteller@cnio.es).

Published online 13 March 2005; doi:10.1038/ng1531

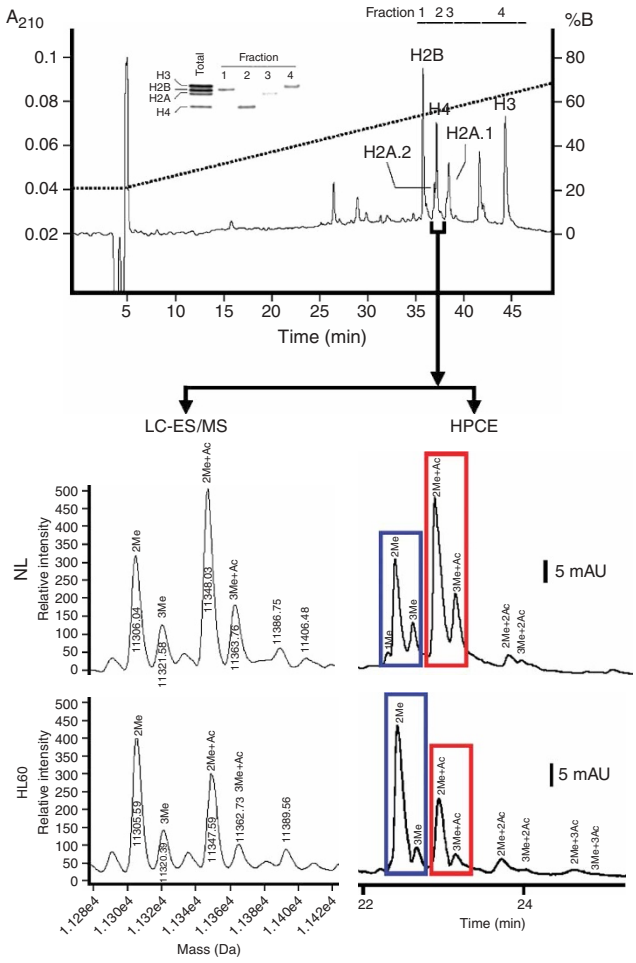

Figure 1 Quantification of global histone H4 post-translational modifications. Core histones were separated by reverse-phase HPLC. A_{210}, absorbance at 210 nm; %B, concentration of solvent B (acetonitrile). A Coomassie blue–stained gel identifying each histone fraction is shown in the square. Histone H4 post-translational modifications were analyzed by LC-ES/MS (left traces) and HPCE (right traces) in normal lymphocytes (NL) and the human cancer cell line HL60. The LC-ES/MS traces are the result of deconvolution analysis of purified histone H4 ion spectra. Selected peaks are labeled by observed average masses and represent post-translational modification by methylation (Me) and acetylation (Ac). Leukemia cells have lower levels of monoacetylated and trimethylated histone H4.

RESULTS

Loss of monoacetylation and trimethylation of H4 in cancer

We first compared histone modification patterns in the tail of histone H4 in normal lymphocytes ($n = 80$) versus transformed cells from leukemia cell lines, such as HL60 and Jurkat. We purified histone H4 using high-performance liquid chromatography (HPLC) and examined the eluted fraction by high-performance capillary electrophoresis (HPCE)[26] and liquid chromatography–electrospray mass spectrometry (LC-ES/MS)[27] (**Fig. 1**). In the HPCE analysis, each of the non-, mono-, di-, tri- and tetra-acetylated histone derivatives appeared as a doublet of peaks (**Fig. 1**). The first and second peaks of the doublet were identified as di- and trimethylated histone H4, respectively, by LC-ES/MS analysis of the same samples (**Fig. 1**).

Both analyses showed marked differences in the patterns of histone H4 modification in normal lymphocytes versus leukemia cell lines (**Fig. 1**). First, there was a relative loss of 60% of the total content of monoacetylated histone H4 (the second doublet of peaks; **Fig. 1**), which appeared in both di- and trimethylated forms, in leukemia cells. Second, there was a relative loss of 75% of the total amount of trimethylated histone H4 (the second peak of each doublet) in the non-, mono-, di- and triacetylated forms (**Fig. 1**) in leukemia cells. We extended the analysis to 25 cancer cell lines corresponding to other tumor types, including breast, lung and colon cancer, and their normal counterparts. We obtained the same profile in all cancer cells: histone H4 lost monoacetylation and trimethylation (**Fig. 2a**).

Because cells grown in culture might not reflect primary cancers, we isolated histone H4 from fresh primary tumors (16 lymphomas and 20 colorectal adenocarcinomas) and from their normal counterparts (tonsils and normal colon mucosa, respectively) and repeated the HPCE and LS-ES/MS analyses. The results of these analyses in primary tumors were very similar to those found in cancer cell lines: in normal tissues, ~60% of total histone H4 was monoacetylated, whereas in primary tumors, only 35% on average was monoacetylated (**Fig. 2a**). We obtained similar findings for trimethylated histone H4: tumor samples showed a relative loss of 50% of trimethylated histone H4 on average compared with corresponding normal tissues (**Fig. 2a**). We also carried out a paired comparison between the colorectal cancer and corresponding normal colon mucosa from each individual ($n = 17$). In all cases, the tumor sample had less monoacetylated and trimethylated histone H4 (**Supplementary Fig. 1** online).

Global histone H4 modification patterns change during the cell cycle, with monoacetylation and trimethylation of H4 declining in metaphase[28,29]. To differentiate this decline from cancer-associated loss, we carried out two different experiments. First, we observed that for nontumorigenic lymphoblastoid cell lines and leukemia cell lines, G0-G1 cells had twice as much monoacetylated and trimethylated H4 than did G2-M cells. In normal and cancer cells both arrested at G0-G1 or G2-M, this relative loss of monoacetylated and trimethylated H4 in tumorigenic cells was still evident (**Fig. 2b** and **Supplementary Fig. 2** online). Second, the relative loss of monoacetylated and trimethylated H4 in malignant cells was maintained even when the doubling time is accounted for, as the leukemia and nontumorigenic lymphoblastoid cells had similar doubling times (**Supplementary Fig. 2**). Moreover, the reactive tonsils had a high rate of cell division and abundant Ki67 labeling, similar to lymphomas, but the tumors showed a loss of monoacetylated and trimethylated H4. Therefore, although a cell-cycle decline in monoacetylation and trimethylation of histone H4 occurs in normal dividing cells, transformed cells are subject to a specific loss.

If the loss of monoacetylation and trimethylation of histone H4 occurs early in the process and becomes more accentuated in more advanced stages, as occurs with genetic lesions[30], CpG island hypermethylation[3,5,6,31] and global genomic hypomethylation[1,2,31], then an association with the malignant phenotype would be more likely. Therefore, we used HPCE to determine the histone H4 modification patterns in a well-defined model of tumor progression, the mouse multistage skin carcinogenesis model[32]. In this model, sequential topical application of various mutagens generates different stages of tumorigenesis. We examined normal mouse skin (NS), benign papilloma cells (PB), tumorigenic squamous carcinoma cells (PDV and PAM212) and the highly anaplastic and metastatic spindle carcinoma cell lines (MSC11A5, CarB and CarC). We found that the loss of monoacetylation and trimethylation of histone H4 was an early event: it had already occurred in benign papillomas (**Fig. 2c**) and was progressively lost from these early stages through to the most malignant stages.

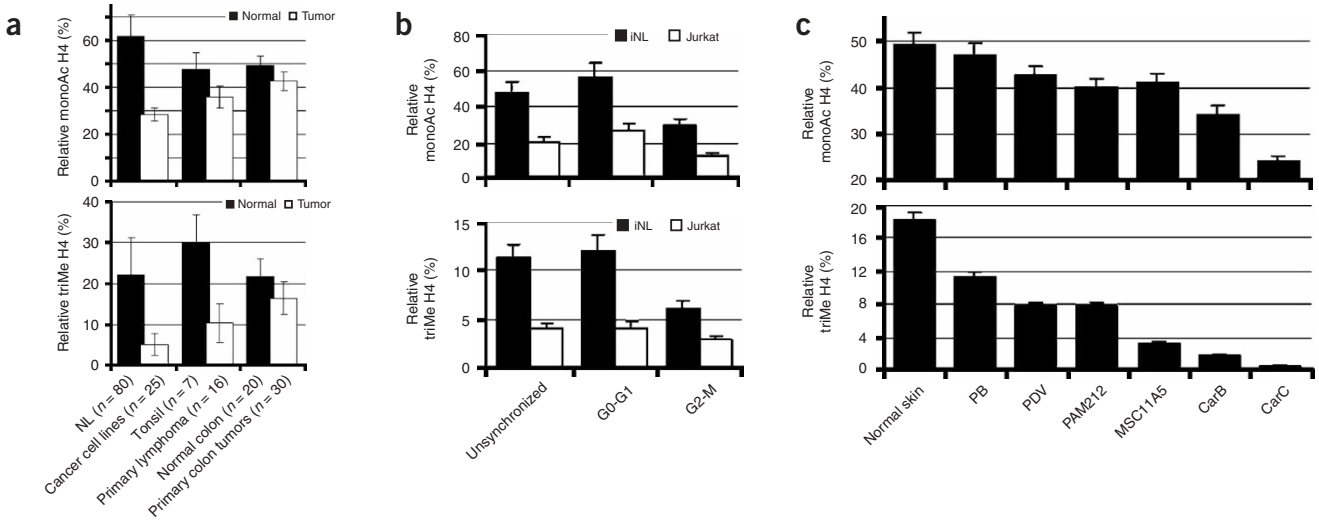

Figure 2 Loss of monoacetylation and trimethylation of histone H4 occurs in cancer. (**a**) Relative levels of monoacetylated (monoAc; upper panel) and trimethylated (triMe; lower panel) histone H4 in cancer samples (open bars) versus their normal counterparts (filled bars) quantified by HPCE. (**b**) HPCE quantification of the relative levels of monoacetylated (monoAc; upper panel) and trimethylated (triMe; lower panel) histone H4 in immortalized normal lymphocytes (iNL; black bars) and the cancer cell line Jurkat (white bars) in unsynchronized cells and cells synchronized in G0-G1 and G2-M. (**c**) Relative levels of monoacetylated (monoAc; upper panel) and trimethylated (triMe; lower panel) histone H4 in a mouse model of skin multistage tumor progression, quantified by HPCE. The loss of monoacetylation and trimethylation of histone H4 occurs early and accumulates during the tumorigenic process.

Loss of monoacetylation at H4-Lys16 occurs in cancer cells

We next determined which positions in the tail of histone H4 correspond to the loss of monoacetylation. Four lysines are acetylated in the tail of H4: Lys5, Lys8, Lys12 and Lys16. Previous results suggested that the order in which these H4 residues are acetylated is nonrandom: first Lys16, followed by Lys12, then Lys8 and finally Lys5 (refs. 33,34). Therefore, loss of monoacetylation of histone H4 in cancer cells should occur predominantly at Lys16. To determine whether this was the case, we used antibodies against specific acetylated residues of H4 (refs. 28,33) and tandem mass spectrometry[35].

We first used western blotting to assess acetylation at Lys5, Lys8, Lys12 and Lys16 in reactive tonsil (the corresponding normal tissue) and in five human primary lymphomas. In four of the five cases (80%), only Lys16 was hypoacetylated in the lymphomas versus the controls (**Fig. 3a**). This loss of acetylation at Lys16 in the cancer cells was also observed by immunolocalization (**Fig. 3a**). Second, we subjected purified histone H4 from normal lymphocytes and leukemia cells to tryptic digestion and analysis by tandem mass spectrometry (MS/MS; **Fig. 3b**). Normal and cancer cells shared three peptides containing the four acetylated lysines of the histone tail (Lys5, Lys8,

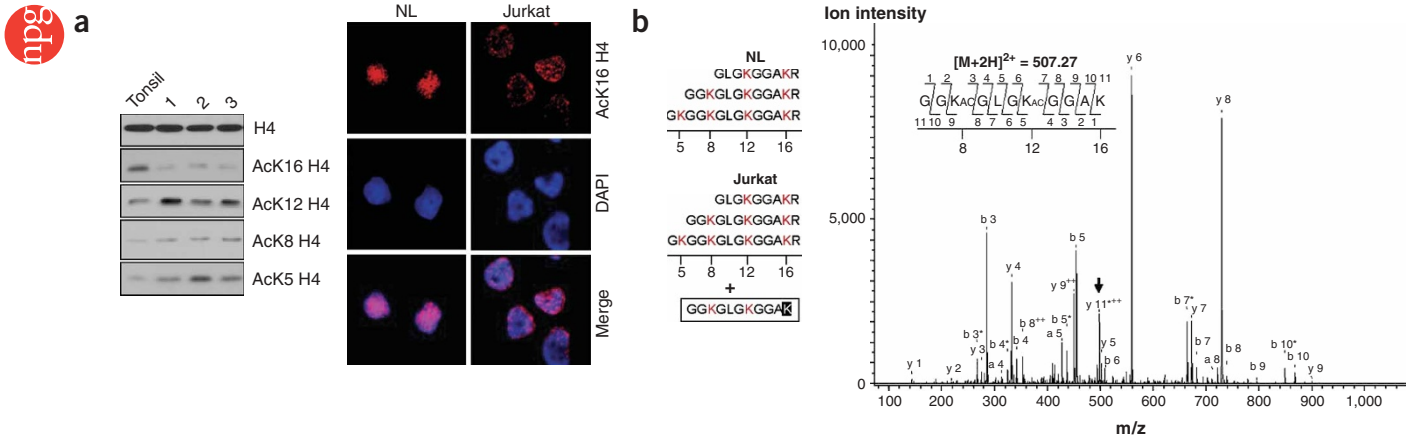

Figure 3 Loss of monoacetylation of histone H4 in cancer cells occurs mainly at Lys16. (**a**) Left panel, western blot comparing specific acetylation modifications of histone H4 in control tissue (Tonsil) versus primary lymphomas (samples 1–3). A global antibody to histone H4 was used as a loading control. Right panel, immunofluorescence analysis of acetylated Lys16 and DAPI-stained DNA in normal lymphocytes and Jurkat cells. Ac, acetylated. (**b**) Left panel, peptides from histone H4 identified by MS/MS in normal lymphocytes (NL) versus Jurkat cells. Leukemia cells contain a unique peptide with deacetylation at Lys16 (shown in the box) that it is not present in normal cells. Acetylated lysines are shown in red; nonacetylated lysines in white with a black background. Right panel, MS/MS spectrum for the cancer-specific peptide with deacetylation at Lys16 (507.27 Da). The spectrum shows ions corresponding to the main fragmentation series (b- and y-series) from the doubly acetylated sequence covering residues 6–16 as GGK^{Ac}GLGK^{Ac}GGAK. Water-loss ions (*) and doubly charged fragments ($^{++}$) are indicated. Numbers below the sequence indicate the position of lysine residues on the histone H4 tail. The signal at 498.27, labeled with an arrow, corresponds to a doubly charged water-loss precursor ion.

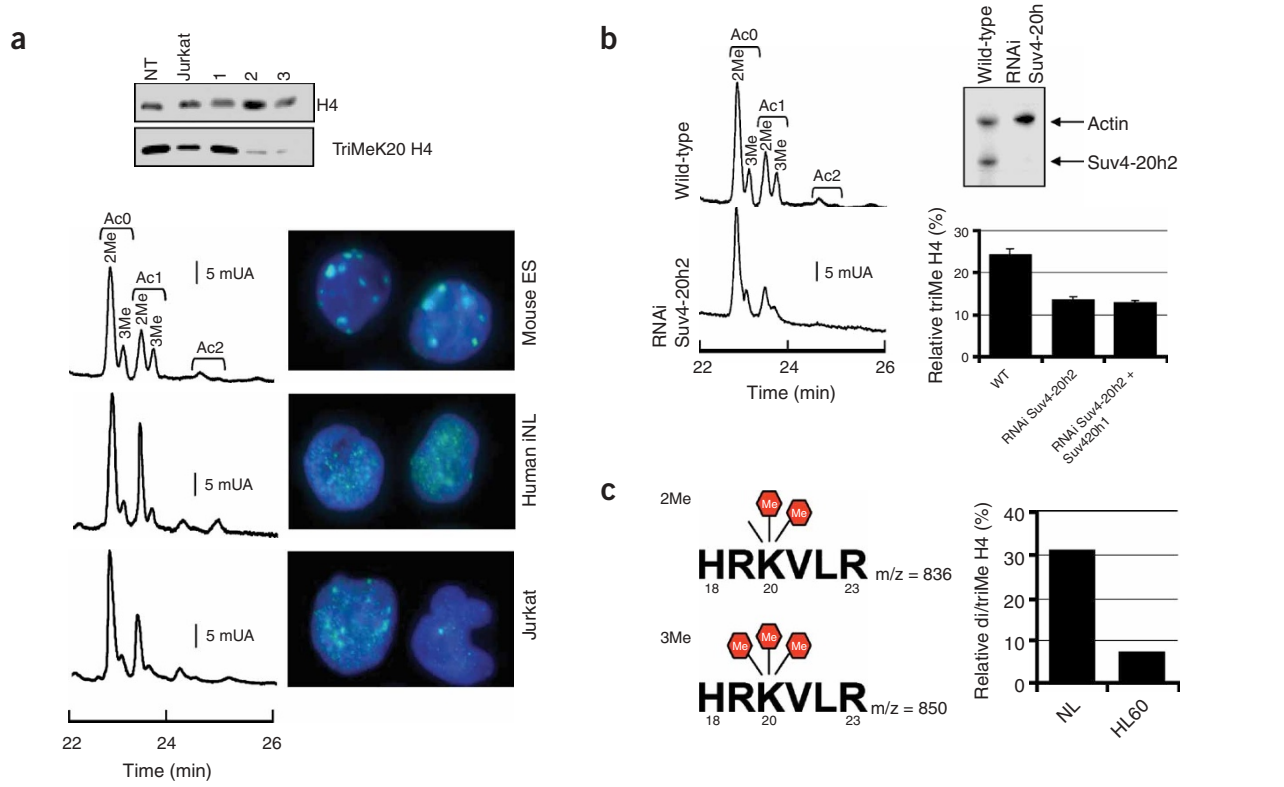

Figure 4 Loss of trimethylation of histone H4 in cancer cells occurs mainly at Lys20. (**a**) Upper panel, western blot comparing specific trimethylation at H4-Lys20 in normal lymphocytes (NT) versus Jurkat cells and primary lymphomas (samples 1–3). Lower panel, quantification of global levels of trimethylated H4-Lys20 by HPCE (left) and double-staining with DAPI and antibody to trimethylated H4-Lys20 (right) in mouse stem cells (ES), lymphocytes (iNL) and Jurkat cells. (**b**) HPCE quantification of histone H4 methylation in control cells and after RNAi for Suv4-20h1 and Suv4-20h2. Left panel, representative electropherograms. Upper panel, western blot for wild-type and Suv4-20h2 knock-down mouse embryonic fibroblasts. Lower panel, quantification of trimethylated H4-Lys20 in these cells. (**c**) Left, Six–amino acid–long peptides containing Lys20 obtained after tryptic digestion of histone H4. Right, relative levels of its trimethylated form in normal lymphocytes (NL) and HL60 cells (right), showing a loss in cancer cells. Ac, acetylated; Me, methylated.

Lys12 and Lys16), but there was an additional peptide specific to leukemia cells: $GGK^{8}GLGK^{12}GGAK^{16}$. This 'cancer-specific' peptide was acetylated at Lys8 and Lys12 but not at Lys16 (**Fig. 3b**). Therefore, loss of acetylation at H4-Lys16 seems to be particular to transformed cells. Finally, we used a third strategy to establish that loss of monoacetylated H4 corresponds to loss of acetylation at H4-Lys16. The colorectal carcinoma cell line HCT-116 had less monoacetylation of H4 than did normal colorectal mucosa (**Supplementary Fig. 3** online). We obtained similar results with other cancer cell lines. We obtained a cell line derived from HCT-116 that has a disruption of the histone acetyltransferase p300 (ref. 36). p300 acetylates histone H4 at Lys5, Lys8 and Lys12 but cannot acetylate Lys16 (ref. 37). In an HPCE assay, similar to the one in which we determined that the loss of acetylation at Lys16 is responsible for the decline in total monoacetylated H4, we found no change in the global monoacetylation status of H4 in p300-knockout HCT-116 cells compared with parental HCT-116 cells (**Supplementary Fig. 3**). These results also imply that the loss of monoacetylation at H4 in malignant cells occurs at Lys16.

Loss of trimethylation at H4-Lys20 occurs in cancer cells

The only lysine in the tail of histone H4 that undergoes methylation is Lys20, which can exist in mono-, di- or trimethylated states[19,27]. To determine whether trimethylation at Lys20 was involved in the decline in trimethylated forms of H4, we used specific antibodies against this modification, HPCE and mass spectrometry.

First, we measured the levels of trimethylated H4-Lys20 in normal lymphocytes and the lymphoma cell line Jurkat by western blotting[17]. The cancer cell line had substantially less trimethylated H4-Lys20 than did normal lymphocytes (**Fig. 4a**). We also carried out immunolocalization experiments, using mouse embryonic fibroblast cells as a positive control[17] (**Fig. 4a**), and observed a decrease in trimethylated H4-Lys20 in the leukemia cell lines compared with normal lymphocytes. Finally, in four of five human primary lymphomas (80%), we again observed this loss of trimethylated H4-Lys20 by western blotting (**Fig. 4a**). We also wished to confirm that the lost second peak of the doublet observed in the HPCE traces corresponded to trimethylated H4-Lys20. To this end, we first knocked-down, by RNA interference (RNAi), Suv4-20h1 and Suv4-20h2, the two histone methyltransferases responsible for trimethylation of histone H4 (ref. 17). The double knock-down reduced the HPCE double peak by 50% (**Fig. 4b**), indicating that it represents trimethylated H4-Lys20. We also used RNAi to knock-down Suv4-20h2 alone, as it has been proposed to be the chief contributor to trimethylation at H4-Lys20, especially at pericentric loci[17]. We determined RNAi efficiency by quantitative RT-PCR (**Supplementary Fig. 4** online) and western blotting (**Fig. 4b**). This single knock-down similarly reduced the HPCE double peak by 50% (**Fig. 4b**), further confirming that it represents trimethylated H4-Lys20. The final indication that the loss of trimethylation of histone H4 in cancer occurs primarily at Lys20 was provided by mass spectrometry. In normal lymphocytes and leukemia cells, we

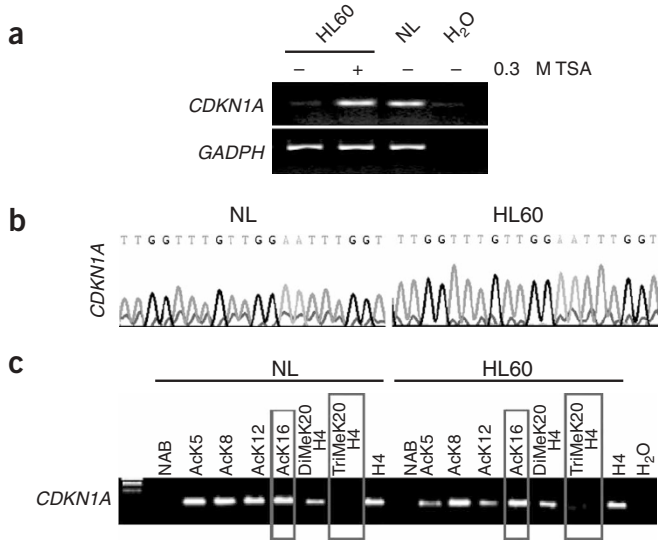

Figure 5 Loss of monoacetylation at H4-Lys16 and trimethylation at H4-Lys20 in cancer cells is not associated with a shift in the histone modification pattern of epigenetically silenced genes. (**a**) Reverse transcription analysis for *CDKN1A* expression. *CDKN1A* is not expressed in HL60 cells, but its expression is restored with trichostatin A (TSA). NL, normal lymphocytes. (**b**) Representative electropherograms of bisulfite-modified DNA from the promoter-containing CpG island of *CDKN1A* show an unmethylated status both in normal lymphocytes (NL) and HL60 cells. (**c**) ChIP analysis of the histone modification status of the *CDKN1A* promoter in normal lymphocytes (NL) and HL60 cells. NAB is the control without antibody. The presence of acetylated Lys16 and trimethylated Lys20 at the *CDKN1A* promoter (shown in their respective boxes) does not change between normal lymphocytes and HL60 cells. Ac, acetylated; Me, methylated.

characterized a six–amino acid–long peptide with Lys20 in the central position: $H^{18}RK^{20}VLR^{23}$ (**Fig. 4c**). We quantified the differentially modified peptides[27] and found that leukemia cells lost 77% of the trimethylated H4-Lys20 found in normal lymphocytes (**Fig. 4c**), providing further evidence that this site is the target for the loss of trimethylation of histone H4.

We also wished to determine whether all the histone H4 monoacetylated at Lys16 or only histone H4 methylated at Lys20 was depleted in the cancer cells. The mass spectrometry spectra showed that loss of monoacetylated H4 in cancer occurred for both dimethylated and trimethylated histones (**Fig. 1**) and that most histone H4 is di- or trimethylated at Lys20 in both normal and cancer cells. Therefore, although monoacetylated histone H4 may exist in the unmethylated H4-Lys20 isoform, the amount is so small that it is at the limit of detection (always $<1\%$). The relative amounts of the eight possible combinations of modifications for Lys16 and Lys20 in normal versus cancer cells is shown in **Supplementary Fig. 5** online.

No association with histone-silenced genes

We wanted to determine at which genomic loci the loss of acetylated H4-Lys16 and trimethylated H4-Lys20 took place in the cancer cells. At least three aberrant epigenetic events occur in transformed cells: the global loss of 5-methylcytosine DNA content, originating mainly from repetitive sequences[1,2,31] and some hypomethylated CpG islands[38]; the hypermethylation of promoter-associated CpG islands of tumor-suppressor genes[3–6]; and a shift in the promoter histone modification pattern without DNA methylation changes, such as occurs with *CDKN1A* (refs. 23,24). We investigated these three possible targets.

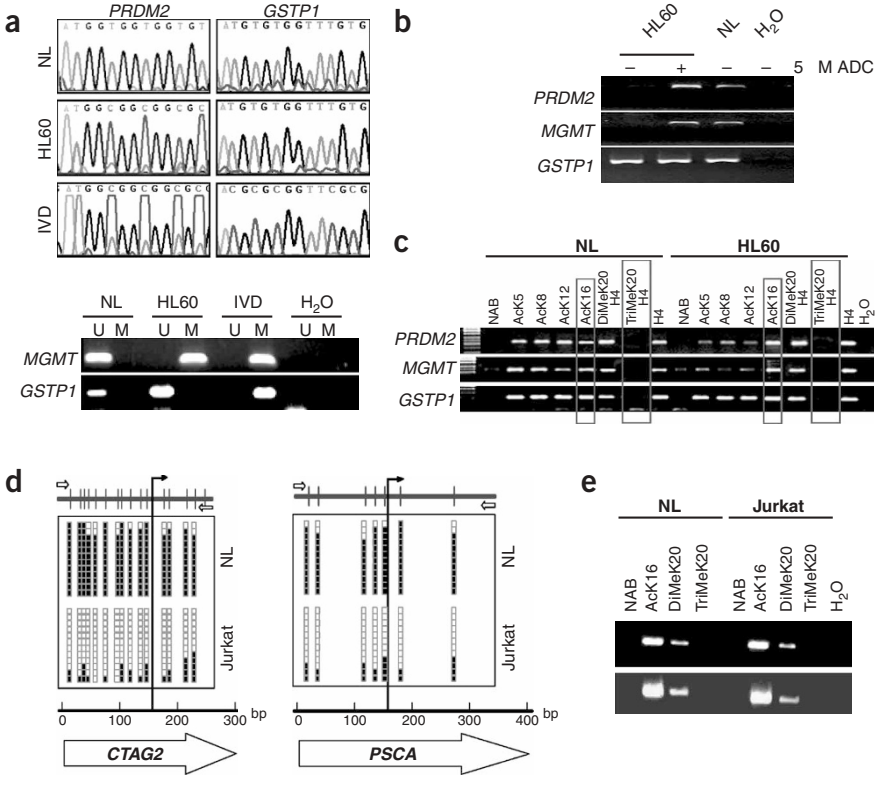

Figure 6 Loss of monoacetylation at H4-Lys16 and trimethylation at H4-Lys20 in cancer cells is not associated with promoter-associated CpG islands. (**a**) Upper panel, Electropherograms of bisulfite-modified DNA from the *PRDM2* and *GSTP1* CpG islands in normal lymphocytes (NL) and HL60 cells. The presence of protected cytosines indicates methylated CpG sites. Lower panel, Methylation-specific PCR analysis. U, unmethylated allele; M, methylated allele. *In vitro*–methylated DNA (IVD) was used as positive methylated control. *PRDM2* and *MGMT* are hypermethylated in HL60 cells and unmethylated in normal lymphocytes. *GSTP1* is unmethylated in HL60 cells and normal lymphocytes. (**b**) Reverse transcription analysis. *PRDM2* and *MGMT* are not expressed in HL60 cells, but expression is restored with ADC. *GSTP1* is expressed in HL60 cells and normal lymphocytes (NL). (**c**) ChIP analysis of the *PRDM2*, *MGMT* and *GSTP1* promoters. The presence of acetylated Lys16 and trimethylated Lys20 (shown in their respective boxes) does not change between normal lymphocytes (NL) and HL60 cells. NAB is the control without antibody. (**d**) Bisulfite genomic sequencing of twelve clones of the *CTAG2* and *PSCA* promoter regions. Filled circles, methylated CpGs; open circles, unmethylated CpGs. (**e**) ChIP analysis of the histone modification status of the *CTAG2* and *PSCA* promoter regions. NAB is the control without antibody. Ac, acetylated; Me, methylated.

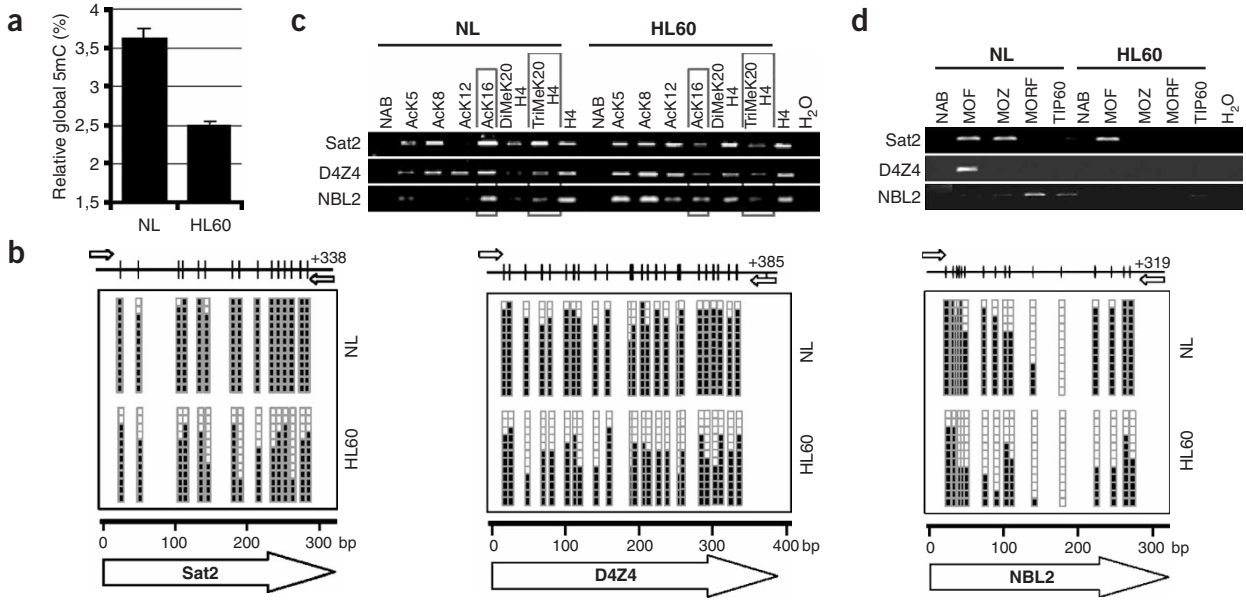

Figure 7 Loss of monoacetylation at H4-Lys16 and trimethylation at H4-Lys20 in cancer cells is associated with DNA hypomethylation of repetitive sequences. (**a**) 5-methylcytosine (5mC) genomic content by HPCE in normal lymphocytes (NL) and HL60 cells as a percentage of the total cytosine pool. (**b**) Bisulfite genomic sequencing of twelve clones of the repetitive DNA sequences Sat2, D4Z4 and NBL2 in normal lymphocytes (NL) and HL60 cells. Filled circles, methylated CpGs; open circles, unmethylated CpGs. All repetitive sequences are hypomethylated in HL60 cells versus normal lymphocytes. (**c**) ChIP analysis of the repetitive DNA sequences in normal lymphocytes (NL) and HL60 cells. Loss of acetylation at H4-Lys16 and trimethylation at H4-Lys20 for Sat2, D4Z4 and NBL2 repetitive sequences (shown in their respective boxes) is observed in leukemia versus normal cells. NAB is the control without antibody. Ac, acetylated; Me, methylated. (**d**) ChIP analysis of the Lys16-specific histone acetyltransferases MOF, MOZ, MORF and TIP60 at the repetitive DNA sequences in normal lymphocytes (NL) and HL60 cells. NAB is the control without antibody.

CDKN1A undergoes epigenetic silencing in cancer cells through a change in the histone modification pattern[23,24]. The presence of global hypoacetylation in the *CDKN1A* promoter, detected using an antibody that recognizes a peptide that is tetra-acetylated at Lys5, Lys8, Lys12 and Lys16, is associated with transcriptional silencing[24]. *CDKN1A* was expressed in normal lymphocytes and lost in leukemia cells but restored by treatment with HDAC inhibitors (**Fig. 5a**). The *CDKN1A* promoter–associated CpG island was always unmethylated (**Fig. 5b**). To assess which acetylation changes occurred at the *CDKN1A* promoter, we used specific antibodies against the four lysine residues in a chromatin immunoprecipitation (ChIP) assay. Lys5 and Lys12 of H4 were hypoacetylated in leukemia cells compared with normal lymphocytes, whereas the acetylation status of Lys8 and Lys16 did not change (**Fig. 5c**). ChIP for trimethylated H4-Lys20 also showed no differences between normal and leukemia cells. These data suggest that the loss of acetylation at H4-Lys16 and trimethylation at H4-Lys20 in cancer cells was not due to *CDKN1A*-like sequences, as an archetype of genes undergoing shifts in the histone modification pattern without DNA methylation changes.

This conclusion was confirmed when we analyzed histone H4 from HL60 cells before and after treatment with HDAC inhibitors. HPCE analysis and western blotting using an antibody raised against a tetra-acetylated peptide showed that sodium butyrate induced global hyperacetylation of histone H4 (**Supplementary Fig. 6** online). HPCE electropherograms also showed that the effect was more pronounced for N-terminal, more exposed lysines, manifested as an increase in tetra-acetylated histones relative to monoacetylated. Using antibodies against specifically acetylated residues, we found that acetylated Lys5 increased by a factor of 50 and acetylated Lys16 increased by a factor of only 1.5 (**Supplementary Fig. 6**). These observation reinforce the idea that of lysine residues on histone H4 undergo ordered acetylation[28]. Because acetylated H4-Lys5 is very rare, its presence is greatly enhanced by the use of HDAC inhibitors; the maximum possible increase in acetylated H4-Lys16 is much less.

No association with CpG island methylation

The second candidate locus at which changes in acetylation at H4-Lys16 and trimethylation at H4-Lys20 could occur in cancer cells is promoter-associated CpG islands: CpG island hypermethylation in tumor-suppressor genes[3–6] or hypomethylation of certain CpG islands[38].

Because we used leukemia cell lines, we selected two genes whose CpG islands are hypermethylated in HL60 cells: the DNA repair gene *MGMT* and the retinoblastoma-interacting protein *PRDM2* (also called *RIZ1*; refs. 4,39). We used glutathione S-transferase P1 (*GSTP1*) as an unmethylated CpG island[4,39]. DNA methylation analysis showed that *MGMT* and *PRDM2* CpG islands were unmethylated in normal lymphocytes and hypermethylated in HL60 cells, whereas *GSTP1* was unmethylated in both (**Fig. 6a**). Expression of *GSTP1* was present in HL60 cells, whereas expression of *MGMT* and *PRDM2* was not detected but was restored with DNA demethylating agents (**Fig. 6b**). ChIP showed that both methylation-silenced genes were hypoacetylated at Lys5, Lys8 and Lys12 of H4 in leukemia cells compared with normal lymphocytes, whereas acetylation at H4-Lys16 did not differ (**Fig. 6c**). Trimethylation at H4-Lys20 also showed no difference between normal lymphocytes and leukemia cells (**Fig. 6c**). Acetylation at Lys5, Lys8, Lys12 and Lys16 and trimethylation at Lys20 for the unmethylated *GSTP1* CpG island was the same in normal lymphocytes and HL60 cells. These results suggest that the loss of

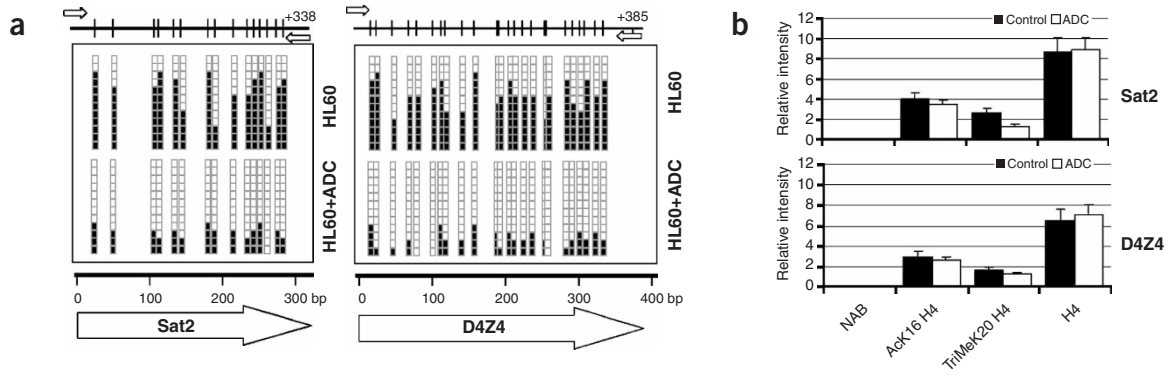

Figure 8 Loss of methylation induced by treatment with demethylating drugs in repetitive Sat2 and D4Z4 sequences is associated with a loss of monoacetylation at H4-Lys16 and trimethylation at H4-Lys20. (**a**) Bisulfite genomic sequencing of twelve clones of the promoter region of the repetitive sequences in HL60 cells after and before treatment with ADC. Filled circles, methylated CpGs; open circles, unmethylated CpGs. (**b**) Densitometric quantifications of triplicate ChIP analysis of the histone modification status (acetylated Lys16, dimethylated Lys20 and trimethylated Lys20) in repetitive Sat2 and D4Z4 sequences in HL60 cells after and before treatment with ADC. NAB is the control without antibody. Ac, acetylated; Me, methylated.

acetylation at H4-Lys16 and trimethylation at H4-Lys20 in transformed cells was not related to CpG island hypermethylation.

A second aspect of aberrant CpG island methylation in cancer is manifested in the hypomethylation of certain CpG islands that are normally methylated in somatic tissues[38]. These include CpG islands in testis-specific genes, melanoma antigens and certain proliferation-linked genes[38]. To determine whether these loci were involved in the altered acetylation at H4-Lys16 and trimethylation at H4-Lys20, we studied eight genes belonging to this category: *MAGEA1*, *CAGE1*, *CTAG2*, *GAGE1*, *PSCA*, *S100A4* and *MSLN*[38]. All their CpG islands were methylated in normal lymphocytes, but only the *CTAG2* and *PSCA* CpG islands were hypomethylated in leukemia cells (**Fig. 6d**). ChIP assay showed no changes in acetylation at H4-Lys16 or trimethylation at H4-Lys20 for these two hypomethylated sequences between normal lymphocytes and leukemia cells, despite the change in DNA methylation (**Fig. 6e**). Therefore, this type of sequence did not contribute to the loss of acetylation at H4-Lys16 and trimethylation at H4-Lys20 in tumor cells.

Association with DNA hypomethylation of repetitive sequences

We next attempted to determine whether the loss of acetylation at H4-Lys16 and trimethylation at H4-Lys20 occurred at the third putative location, the DNA repetitive regions that experience a general loss of DNA methylation in tumorigenesis. Human tumors have a lower genomic content of 5-methylcytosine than their normal counterparts[1,2,31,38,39]. Most of these hypomethylated sites correspond to DNA repetitive sequences[38]. In our model, we also observed that all cancer cell lines and primary tumors were globally unmethylated compared with their respective counterparts. For the leukemia cell line HL60, the genomic content of 5-methylcytosine was 40% lower than in normal lymphocytes (**Fig. 7a**). We next focused on two different types of particular DNA repeat sequences: pericentromeric repeats, such as Sat2, and subtelomeric repeats, such as the nonsatellite repeats D4Z4 and NBL2 (ref. 40). Both types of sequence were hypomethylated in leukemia cells relative to normal lymphocytes: 15% for NBL2, 25% for D4Z4 and 30% for Sat2 (**Fig. 7b**). ChIP analysis showed that whereas Lys5, Lys8 and Lys12 were hyperacetylated in the leukemia cells, Lys16 was markedly hypoacetylated (**Fig. 7c**). Furthermore, the different behavior of Lys16 in the transformed cells with respect to these DNA repetitive regions occurred in conjunction with a loss of trimethylation at H4-Lys20 for all the repeat sequences in the leukemia cells (**Fig. 7c**). Treatment of the leukemia cell line with the DNA demethylating agent 5-aza-2′-deoxycytidine (ADC) caused further DNA hypomethylation and greater reduction in acetylation at H4-Lys16 and trimethylation at H4-Lys20 at these repeat sequences (**Fig. 8**).

Finally, we sought to identify proteins deregulated in transformed cells that could account for the observed loss of acetylation at H4-Lys16. Acetylation at H4-Lys16 is tightly regulated, and several histone acetyltransferases are involved, including MOF, MORF, MOZ and TIP60 (ref. 41). A direct connection with tumorigenesis has already been established, as the genes encoding MOZ and MORF are common fusion partners in chromosomal translocations associated with hematological malignancies[41]. First, we studied two specific leukemia samples: one carrying the MOZ-CBP translocation and another carrying the MORF-CBP translocation. The MOZ-CBP fusion protein was associated with a global loss of acetylation at H4-Lys16, similar to that observed for leukemia cell lines. But the MORF-CBP translocation was associated with extremely low levels of acetylation at H4-Lys16, suggesting that MORF has an important role in the modification of Lys16 (**Supplementary Fig. 7** online). We also used ChIP to assess differential occupation of the studied repeat regions by these histone acetyltransferases. We observed a sequence-specific loss of Lys16 acetyltransferase recruitment in leukemia cells compared with normal lymphocytes: MORF was lost at NBL2, MOZ at Sat2 and MOF at D4Z4 (**Fig. 7d**).

These findings lead us to propose that the loss of acetylation at H4-Lys16 and trimethylation at H4-Lys20 in tumor cells occurs in repetitive DNA sequences, in association with the global loss of DNA methylation common in tumorigenesis.

DISCUSSION

Great effort has been devoted to understanding the relevance of aberrant DNA methylation patterns in human tumors. Two apparently opposite phenomena coexist: a profound loss of global genomic content of 5-methylcytosine with discrete areas of dense hypermethylation[3–6,38,42]. Overall, hypomethylation take places predominantly in DNA repetitive sequences[38] and may be linked to chromosomal instability[43,44]. On the other hand, hypermethylation occurs in the CpG islands located in the promoters of certain tumor-suppressor genes such as *CDKN2A*, *BRCA1* and *MLH1* (refs. 3–6). But DNA methylation is just one of the many layers of epigenetic control[38,42].

Histones are another key player. They have a primordial role in the control of gene expression and chromatin structure[10,11], together with DNA methylation[9,10]. But our knowledge of the behavior of histones in cancer is poor. Apart from the role of certain histone modifications in gene silencing, with[20–22] or without[23,24] CpG island hypermethylation, there has previously been no portrait available of general aberrant histone modification patterns in cancer cells. Here, we show that human tumors undergo an overall loss of monoacetylation at H4-Lys16 and trimethylation at H4-Lys20. These two losses can be considered almost universal epigenetic markers of malignant transformation, like global DNA hypomethylation and CpG island hypermethylation.

Changes in histone modifications affect DNA methylation[45], but changes in DNA methylation also affect histone modifications[40,46]. We found that the loss of acetylation at H4-Lys16 and trimethylation at H4-Lys20 could be assigned to DNA repetitive regions that undergo DNA hypomethylation in cancer cells. Therefore, these hypomethylated loci could drive the observed chromatin changes. We do not know which occurs first, but these genomic regions have profoundly disturbed epigenetic regulation with regard to both DNA methylation and histone modification. These findings should inspire us to study how the chromatin domains of the cancer cell genome become misplaced. Defects in the establishment of DNA methylation patterns may be related to the generation of genomic aberrations[43,44], but perhaps an imbalanced pattern of histone modifications could also be invoked.

The identities of the molecules responsible for the aberrant profile of histone H4 modifications are of note. We found a loss of recruitment of the H4-Lys16 acetyltransferases MOZ, MOF and MORF to repeat sequences in cancer cells and an association of the fusion proteins MOZ-CBP and MORF-CBP with substantial global losses of acetylation at H4-Lys16. The other partner of the fusion protein is usually CBP or p300, both histone acetyltransferases with numerous substrates that do not act on H4-Lys16 (refs. 37,41). Similarly, the deacetylation of H4-Lys16 seems to be closely regulated: in yeast, SIR2 deacetylates this residue; its human homolog, Sirtuin 1 (SIRT1), also deacetylates the tumor-suppressor protein p53 (ref. 47), thereby establishing another link with cancer. A similar scenario could be conceived for trimethylation at H4-Lys20. Two human histone methyltransferases, Suv4-20h1 and Suv4-20h2, are responsible for methylation at Lys20 (ref. 17), in addition to PR/SET7 and SET8 (refs. 48,49). They could also constitute targets for disruption in cancer cells, as occurs with another histone methyltransferase, MLL, which is translocated in hematological malignancies[50]. These results reinforce the idea that aberrant histone modification patterns have a role in the tumorigenic process.

Our results suggest a global aberrant pattern of histone H4 modification associated with the transformed phenotype. This histone H4 'cancer signature' is characterized by a loss of monoacetylation at Lys16 and trimethylation at Lys20, predominantly located at DNA repetitive sequences. These findings may have implications for the identification of histone-modifying enzymes as putative targets for cellular transformation, for the development of histone-related biomarkers of cancer and for a better understanding of the inhibitors of HDACs as antitumor agents.

METHODS

Cell lines and primary tumor samples. We obtained 25 human cancer cell lines corresponding to leukemia (HL60, Jurkat, K562 and REH), lymphoma (Raji, U937, Molt16, HT and HuT78), breast (MDA-MB-231 and MCF-7), colon (HCT-116, LoVo, RKO and Colo-205), bone (A637 and MG63), cervix (SiHa, CaSki and SK-N-SH), lung (H1299), testis (NTERA), neuroblastoma (SKN-SH), osteosarcoma (MG63) and prostate (LnCAP) cell types from the American Type Culture Collection and the German Collection of Microorganisms and Cell Cultures. The origin of the mouse multistage skin cancer model cells was previously described[31,32]. The p300 knock-out cells used were previously described. We obtained them by homologous recombination targeting exon 2 of the gene *EP300* (ref. 36). To reactivate *CDKN1A*, we carried out HDAC inhibition treatment by adding 0.3 μM trichostatin A to the culture medium for 24 h or by treating the cells for 6 h in medium supplemented with 10 mM sodium butyrate (Sigma)[33]. We carried out demethylating treatments using ADC (1 μM) for 48 h, replacing the drug and medium 24 h after the beginning of the treatment. For the cell cycle experiments, we synchronized cells at G0-G1 and G2-M by serum starvation and nocodazole treatment, respectively. For serum starvation, we incubated actively growing Jurkat and lymphoblastoid cell lines for 24 h in RPMI medium supplemented with 0.5% fetal bovine serum. To arrest cell cultures in G2-M, we incubated subconfluent Jurkat and lymphoblastoid cells for 18 h in RPMI medium plus 10% fetal bovine serum containing 500 ng ml^{-1} nocodazole. After treatment, we washed cells and incubated them in the absence of nocodazole for 2 h. We confirmed cell-cycle profiles of synchronized cell lines by flow cytometry. We obtained tissue samples of 36 human primary malignancies corresponding to lymphoma ($n = 16$) and colon carcinomas ($n = 20$), as well as normal tonsils ($n = 3$) and normal colon mucosa ($n = 5$), at the time of clinically indicated surgical procedures from the Tumor Bank of the Spanish National Cancer Center. From 17 individuals with colorectal cancer we obtained a normal sample and a tumor sample. We obtained 80 normal lymphocytes from healthy volunteers.

Histone extraction. We prepared histone in accordance with established protocols[28]. We obtained histones from cell lines and tumor samples in parallel with their matching controls under identical conditions. For cell lines, we isolated nuclei with RSB buffer (10 mM Tris 10 (pH 7.5), 10 mM NaCl and 3 mM $MgCl_2$) containing 1% Nonidet-P40 and protease inhibitors. We extracted nuclei with 0.25 M HCl and precipitated them with eight volumes of acetone. For tumors and their normal tissue counterparts, we homogenized samples with a Polytron homogenizer (Brinkman Instruments) in 0.25 M HCl and incubated them with gentle agitation for 4 h. We precipitated the resulting supernatant with eight volumes of acetone. We then fractionated individual histones by reverse-phase HPLC on a Jupiter C18 column. We made comparisons only between samples extracted with identical methodology.

Western blotting and immunolocalization. For western blotting, we collected cells by centrifugation and washed cell pellets twice with phosphate-buffered saline buffer. We then extracted the histones directly from the cell pellets with 0.250 M HCl. We fractionated 10 μg of the acid-extracted proteins on a 10% SDS-PAGE gel, transferred the fractions to a polyvinylidene difluoride membrane with 22-μm pore size (Immobilon P^{SQ}, Millipore), blocked the membrane in 5% milk PBS-T (phosphate-buffered saline with 0.1% Tween-20) and immunoprobed it with antibodies to acetylated H4-Lys12 (1:2,000), dimethylated H4-Lys20 (1:2,000) or trimethylated H4-Lys20 (1:1,000; all from Upstate) and with antibodies to acetylated H4-Lys5 (1:1,000), acetylated H4-Lys8 (1:1,000) and acetylated H4-Lys16 (1:4,000; all from Abcam). We used horseradish peroxidase–conjugated antibody to rabbit IgG (Amersham) at 1:3,000 dilution in PBS-T as the secondary antibody and antibody to H4 (1:3,000; Upstate) as a loading control. We raised Suv4-20h2 antibodies in rabbits using a linear peptide corresponding to amino acid residues 10–24 (ELCENDDLATSLVLD) of human Suv4-20h2 (Abcam ab18186). We detected signals with a Luminol reagent detection kit (Santa Cruz Biotechnology, Inc.). For immunolocalization experiments, we grew cells on coverslips and stained them with a mouse antibody against acetylated H4-Lys16 (Abcam) as previously described[40]. We obtained images with a Leica DMRD photomicroscope coupled to a Leica DC200 camera, processed them using Adobe Photoshop software and analyzed them using public National Institutes of Health Image software. We measured indirect immunofluorescence of total trimethylated H4-Lys20 in interphase cells as previously described[17], using antibody against trimethylated H4-Lys20 (Upstate). All samples were analyzed in triplicate. We carried out densitometric quantification using Quantity One Software (BIO-RAD; data available on request).

ChIP. We carried out ChIP assays as previously described[22] with the same antibodies as used for the western blotting (5 μg per 10^6 cells). We sheared chromatin sheared to an average length of 0.2–0.5 kb for this analysis. We carried out PCR amplification in 25-μl reactions with primers specific for each of the analyzed promoters. For each promoter, we evaluated the sensitivity of PCR amplification by serial dilution of total DNA collected after sonication (input fraction). Primers and conditions for each DNA sequence are available on request. All samples were analyzed in triplicate. We carried out densitometric quantification using Quantity One Software (BIO-RAD; data available on request).

HPCE quantification of global histone acetylation and methylation. We quantified global histone H4 acetylation and methylation as previously described[40]. We prepared individual histone fractions from cell nuclei and purified them by reverse-phase HPLC on a Jupiter C18 column (Phenomenex, Inc.) with an acetonitrile gradient (20–60%) in 0.3% trifluoroacetic acid using an HPLC gradient system (Beckman-Coulter). We resolved non-, mono, di-, tri- and tetra-acetylated, as well as di- and trimethylated, histone H4 derivatives by HPCE. We used an uncoated fused-silica capillary (Beckman-Coulter; 60.2 cm × 75 μm, effective length = 50 cm) in a capillary electrophoresis system (P/ACE MDQ, Beckman-Coulter) with 100 mM phosphate buffer (pH 2.0) 0.02% (w/v) HPM-cellulose as running buffer and operating voltages of 12 kV.

Analysis of modified histone H4 by LC-ES/MS. We acidified purified histone H4 samples (~1 mg) by adding formic acid to 1% (w/v) and loaded them onto a fused silica column (10 cm × 500 mm internal diameter) packed with POROS 20 R1 perfusion chromatography resin (LC Packings, Inc.). We eluted bound proteins with a gradient of 0–48% (v/v) acetonitrile for 1 h and then 48–80% (v/v) acetonitrile for 20 min in 0.1% (w/v) formic acid and analyzed them by ES/MS. We collected spectra using an ABI QSTAR Pulsar mass spectrometer (Applied Biosystems) and derived deconvolution plots from the ion spectra using Bayesian Protein Reconstruction (ABI Analyst QS software, Applied Biosystems).

MS/MS analysis of amino acid–specific acetylation in histone H4 tail. We incubated purified histone H4 in 50 mM NH_4HCO_3 with 45 μg/ml of trypsin (Promega) at 37 °C for 1 h. We cleaned tryptic peptides on C18 reverse-phase self-packing cartridges (Discovery BIO Wide pore, Supelco) in accordance with the manufacturer's instructions. We then injected samples on-line onto a C18 reverse-phase nanocolumn in an automated nanogradient generator (Ultimate nano-HPLC, LC Packings) controlled by Hystar 2.3 software and analyzed in a continuous acetonitrile gradient consisting of 0–50% A solution (0–50% acetonitrile and 0.5% acetic acid in water) for 45 min and then 50–90% A solution for 1 min. We used a flow rate of ~300 nl min^{-1} to elute peptides from the reverse-phase nanocolumn to a PicoTip emitter nanospray needle (New Objective) for real-time ionization and peptide fragmentation on an Esquire HCT ion-trap (Bruker Daltonics, Inc.) mass spectrometer. We acquired one MS/MS spectrum every second with a 3-Da window (precursor m/z 1.5), 0.90-V fragmentation amplitude and 0.3-min dynamic exclusion time. We batch-processed MS/MS spectra using DataAnalysis 5.1 SR1 and BioTools 2.0 software packages (Bruker Daltonics, Inc.) and searched for them in the MSDB protein database using MASCOT software (Matrix Science).

Mass spectrometry of propionyl-modified histone H4 tail. We separated ~200 pmol of acid-extracted histones by SDS-PAGE, excised the Coomassie-stained bands corresponding to histone H4 and subjected them to chemical modification to derive free amino groups of lysine residues. We digested them overnight with 100 ng of sequencing-grade trypsin (Promega) in a total volume of 40 μl in accordance with the manufacturer's protocol. We acquired MALDI spectra as described[27]. To identify specific post-translational modifications, we analyzed the resulting spectra with the support of MASCOT software. To quantify the differentially modified peptides, we monoisotoped and integrated the corresponding peaks. We took the total cluster area of the different isoforms of one peptide as 100% and determined the contribution of each isoform to the total from the integrated area under each peak.

Semi-quantitative RT-PCR expression analyses. We reverse-transcribed total RNA (2 mg) treated with DNase I (Ambion) using oligo(dT)12–18 primer with Superscript II reverse transcriptase (Gibco/BRL). We carried out PCR reactions in a 20-μl volume containing 1× PCR buffer (Gibco/BRL), 1.5 mM of $MgCl_2$, 0.3 mM of dNTP, 0.25 μM of each primer and 2 U of *Taq* polymerase (Gibco/BRL). We used 100 ng of cDNA for PCR amplification and amplified all of the sequences with multiple cycle numbers (20–35 cycles) to determine the appropriate conditions for identifying semi-quantitative differences in their expression levels. We designed RT-PCR primers for gene sequences between different exons to avoid any amplification of DNA. We also carried out PCR with *GAPDH* (25 and 28 cycles) to ensure cDNA quality and loading accuracy. Primer sequences are shown in **Supplementary Table 1** online.

Analysis of gene promoter methylation. We established the CpG island DNA methylation status by PCR analysis after bisulfite modification[22,39] and then carried out bisulfite genomic sequencing and methylation-specific PCR as described[22,39]. We designed all bisulfite genomic sequencing and methylation-specific PCR primers to encompass the transcription start sites of the genes investigated. Primer sequences are shown in **Supplementary Table 1**.

Quantification of global DNA methylation degree. We determined 5-methylcytosine genomic content by HPCE as previously described[39]. We boiled genomic DNA samples and treated them with nuclease P1 (Sigma) for 16 h at 37 °C and then with alkaline phosphatase (Sigma) for an additional 2 h at 37 °C. After hydrolysis, we measured total cytosine and 5-methylcytosine content by capillary electrophoresis using a P/ACE MDQ system (Beckman-Coulter). Relative 5-methylcytosine content is expressed as a percentage of total cytosine content (methylated and nonmethylated).

Suv4-20h1 and Suv420h2 RNAi knock-down. We generated Suv4-20h knock-downs as described[17]. We cloned DNA oligos containing the 19-mer targeting sequence, a loop region and *Hin*dIII-*Bgl*II restriction sites into pSUPER. For each target gene we used two different 19-mer sequences. We plated mouse embryonic fibroblasts onto 15-cm dishes before transfection and transfected cells with a mixture of 20 μg pSUPER plasmids containing the 19-mer targeting sequences and 2 μg pEGFP-N1 using Lipofectamine (Invitrogen). One day after transfection, we applied selection medium containing 600 μg ml^{-1} G418 to the cells. Five days after transfection, we washed and centrifuged cells and then stored pellets at −80 °C until histone extraction.

Note: Supplementary information is available on the Nature Genetics website.

ACKNOWLEDGMENTS

We thank H. Lindner for advice regarding the optimization of the capillary electrophoresis method for quantification of histone H4 modifications and the Tumor Bank of the Spanish National Cancer Center for providing human primary tumor samples. This work was supported by the Health and Science Departments of the Spanish Government. M.F.F. is funded by the Spanish Association Against Cancer.

COMPETING INTERESTS STATEMENT

The authors declare that they have no competing financial interests.

Received 13 December 2004; accepted 31 January 2005
Published online at http://www.nature.com/naturegenetics/

1. Feinberg, A.P. & Vogelstein, B. Hypomethylation distinguishes genes of some human cancers from their normal counterparts. *Nature* **301**, 89–92 (1983).
2. Goelz, S.E., Vogelstein, B., Hamilton, S.R. & Feinberg, A.P. Hypomethylation of DNA from benign and malignant human colon neoplasms. *Science* **228**, 187–190 (1985).
3. Jones, P.A. & Laird, P.W. Cancer epigenetics comes of age. *Nat. Genet.* **21**, 163–167 (1999).
4. Esteller, M., Corn, P.G., Baylin, S.B. & Herman, J.G. A gene hypermethylation profile of human cancer. *Cancer Res.* **61**, 3225–3229 (2001).
5. Esteller, M. CpG island hypermethylation and tumor suppressor genes: a booming present, a brighter future. *Oncogene* **21**, 5427–5440 (2002).
6. Herman, J.G. & Baylin, S.B. Gene silencing in cancer in association with promoter hypermethylation. *N. Engl. J. Med.* **349**, 2042–2054 (2003).
7. Esteller, M. DNA methylation and cancer therapy: new developments and expectations. *Curr. Opin. Oncol.* **17**, 55–60 (2005).

8. Cedar, H. DNA methylation and gene activity. *Cell* **53**, 3–4 (1988).
9. Dobosy, J.R. & Selker, E.U. Emerging connections between DNA methylation and histone acetylation. *Cell. Mol. Life Sci.* **58**, 721–727 (2001).
10. Bannister, A.J. & Kouzarides, T. Histone methylation: recognizing the methyl mark. *Methods Enzymol.* **376**, 269–288 (2004).
11. Jenuwein, T. & Allis, C.D. Translating the histone code. *Science* **293**, 1074–1080 (2001).
12. Keohane, A.M., O'Neill, L.P., Belyaev, N.D., Lavender, J.S. & Turner, B.M. X-Inactivation and histone H4 acetylation in embryonic stem cells. *Dev. Biol.* **180**, 618–630 (1996).
13. Lunyak, V.V. *et al.* Corepressor-dependent silencing of chromosomal regions encoding neuronal genes. *Science* **298**, 1747–1752 (2002).
14. Belyaev, N., Keohane, A.M. & Turner, B.M. Differential underacetylation of histones H2A, H3 and H4 on the inactive X chromosome in human female cells. *Hum. Genet.* **97**, 573–578 (1996).
15. Suka, N., Suka, Y., Carmen, A.A., Wu, J. & Grunstein, M. Highly specific antibodies determine histone acetylation site usage in yeast heterochromatin and euchromatin. *Mol. Cell* **8**, 473–479 (2001).
16. Kurdistani, S.K., Tavazoiem, S. & Grunstein,, M. Mapping global histone acetylation patterns to gene expression. *Cell* **117**, 721–733 (2004).
17. Schotta, G. *et al.* A silencing pathway to induce H3-K9 and H4-K20 trimethylation at constitutive heterochromatin. *Genes Dev.* **18**, 1251–1262 (2004).
18. Kourmouli, N. *et al.* Heterochromatin and tri-methylated lysine 20 of histone H4 in animals. *J Cell. Sci.* **117**, 2491–2501 (2004).
19. Sarg, B., Koutzamani, E., Helliger, W., Rundquist, I. & Lindner, H.H. Postsynthetic trimethylation of histone H4 at lysine 20 in mammalian tissues is associated with aging. *J Biol. Chem.* **277**, 39195–39201 (2002).
20. Fahrner, J.A., Eguchi, S., Herman, J.G. & Baylin, S.B. Dependence of histone modifications and gene expression on DNA hypermethylation in cancer. *Cancer Res.* **62**, 7213–7218 (2002).
21. Nguyen, C.T. *et al.* Histone H3-lysine 9 methylation is associated with aberrant gene silencing in cancer cells and is rapidly reversed by 5-aza-2′-deoxycytidine. *Cancer Res.* **62**, 6456–6461 (2002).
22. Ballestar, E. *et al.* Methyl-CpG binding proteins identify novel sites of epigenetic inactivation in human cancer. *EMBO J.* **22**, 6335–6345 (2003).
23. Archer, S.Y., Meng, S., Shei, A. & Hodin, R.A. p21(WAF1) is required for butyrate-mediated growth inhibition of human colon cancer cells. *Proc. Natl. Acad. Sci. USA* **95**, 6791–6796 (1998).
24. Richon, V.M., Sandhoff, T.W., Rifkind, R.A. & Marks, P.A. Histone deacetylase inhibitor selectively induces p21WAF1 expression and gene-associated histone acetylation. *Proc. Natl. Acad. Sci. USA* **97**, 10014–10019 (2000).
25. Richon, V.M. *et al.* Histone deacetylase inhibitors: assays to assess effectiveness in vitro and in vivo. *Methods Enzymol.* **376**, 199–205 (2004).
26. Lindner, H., Helliger, W., Dirschlmayer, A., Jaquemar, M. & Puschendorf, B. High-performance capillary electrophoresis of core histones and their acetylated modified derivatives. *Biochem. J.* **283**, 467–471 (1992).
27. Galasinski, S.C., Resing, K.A. & Ahn, N.G. Protein mass analysis of histones. *Methods* **31**, 3–11 (2003).
28. Turner, B.M. & Fellows, G. Specific antibodies reveal ordered and cell-cycle-related use of histone-H4 acetylation sites in mammalian cells. *Eur. J. Biochem.* **179**, 131–139 (1989).
29. Baxter, J. *et al.* Histone hypomethylation is an indicator of epigenetic plasticity in quiescent lymphocytes. *EMBO J.* **23**, 4462–4472 (2004).
30. Fearon, E.R. & Vogelstein, B. A genetic model for colorectal tumorigenesis. *Cell* **61**, 759–767 (1990).
31. Fraga, M.F. *et al.* A mouse skin multistage carcinogenesis model reflects the aberrant DNA methylation patterns of human tumors. *Cancer Res.* **64**, 5527–5534 (2004).
32. Balmain, A. & Harris, C.C. Carcinogenesis in mouse and human cells: parallels and paradoxes. *Carcinogenesis* **21**, 371–377 (2000).
33. Turner, B.M., O'Neill, L.P. & Allan, I.M. Histone H4 acetylation in human cells. Frequency of acetylation at different sites defined by immunolabeling with site-specific antibodies. *FEBS Lett.* **253**, 141–145 (1989).
34. Thorne, A.W., Kmiciek, D., Mitchelson, K., Sautiere, P. & Crane-Robinson, C. Patterns of histone acetylation. *Eur. J. Biochem.* **193**, 701–713 (1990).
35. Zhang, K. *et al.* Histone acetylation and deacetylation: identification of acetylation and methylation sites of HeLa histone H4 by mass spectrometry. *Mol. Cell Proteomics* **1**, 500–508 (2002).
36. Iyer, N.G. *et al.* p300 regulates p53-dependent apoptosis after DNA damage in colorectal cancer cells by modulation of PUMA/p21 levels. *Proc. Natl. Acad. Sci. USA* **101**, 7386–7391 (2004).
37. Schiltz, R.L. *et al.* Overlapping but distinct patterns of histone acetylation by the human coactivators p300 and PCAF within nucleosomal substrates. *J. Biol. Chem.* **274**, 1189–1192 (1999).
38. Feinberg, A.P. & Tycko, B. The history of cancer epigenetics. *Nat. Rev. Cancer* **4**, 143–153 (2004).
39. Paz, M.F. *et al.* A systematic profile of DNA methylation in human cancer cell lines. *Cancer Res.* **63**, 1114–1121 (2003).
40. Espada, J. *et al.* Human DNA methyltransferase 1 is required for maintenance of the histone H3 modification pattern. *J. Biol. Chem.* **279**, 37175–37184 (2004).
41. Yang, X.J. The diverse superfamily of lysine acetyltransferases and their roles in leukemia and other diseases. *Nucleic Acids Res.* **32**, 959–976 (2004).
42. Cho, K.S., Elizondo, L.I. & Boerkoel, C.F. Advances in chromatin remodelling and human disease. *Curr. Opin. Genet. Dev.* **14**, 308–315 (2004).
43. Eden, A., Gaudet, F., Waghmare, A. & Jaenisch, R. Chromosomal instability and tumors promoted by DNA hypomethylation. *Science* **300**, 455 (2003).
44. Ehrlich, M. DNA hypomethylation, cancer, the immunodeficiency, centromeric region instability, facial anomalies syndrome and chromosomal rearrangements. *J. Nutr.* **132**, 2424S–2429S (2002).
45. Tamaru, H. & Selker, E.U. A histone H3 methyltransferase controls DNA methylation in Neurospora crassa. *Nature* **414**, 277–283 (2001).
46. Bachman, K.E. *et al.* Histone modifications and silencing prior to DNA methylation of a tumor suppressor gene. *Cancer Cell* **3**, 89–95 (2003).
47. Vaziri, H. *et al.* hSIR2(SIRT1) functions as an NAD-dependent p53 deacetylase. *Cell* **107**, 149–159 (2001).
48. Nishioka, K. *et al.* PR-Set7 is a nucleosome-specific methyltransferase that modifies lysine 20 of histone H4 and is associated with silent chromatin. *Mol. Cell* **9**, 1201–1213 (2002).
49. Fang, J. *et al.* Purification and functional characterization of SET8, a nucleosomal histone H4-lysine 20-specific methyltransferase. *Curr. Biol.* **9**, 1086–1099 (2002).
50. Nakamura, T. *et al.* ALL-1 is a histone methyltransferase that assembles a super-complex of proteins involved in transcriptional regulation. *Mol. Cell* **10**, 1119–1128 (2002).